Research Journal of Recent Sciences ISSN 2277-2502
Vol. **14(3),** 1-13, July **(2025)** *Res. J. Recent Sci.*

Pyrolysis of Plastic Bags from Household Waste

Melhyas KPLE[1*], Grâce CHIDIKOFAN[2], Maurel AZA-GNANDJI[1], Guevara NONVIHO[3,4], Gontrand BAGAN[1], Hyppolite AGADJIHOUEDE[1], Aristide HOUNGAN[4], Pierre GIRODS[5] and Yann ROGAUME[5]
[1]Laboratory of Rural Engineering, National University of Agriculture (LGR/UNA), 01 BP 55 Porto Novo, Benin
[2]laboratory of Engineering Sciences and Applied Mathematics, National University of Science Technology Engineering and Mathematics, Abomey, Benin
[3]Research Unit on Molecular Interactions, Study and Research Laboratory in Applied Chemistry of the Polytechnic School of Abomey-Calavi, University of Abomey-Calavi (URIM/LERCA/ EPAC/UAC), 01 BP 2009 Cotonou, Benin
[4]Pluridisciplinary Research Laboratory for Technical Education (LARPET), National University of Science Technology Engineering and Mathematics, BP 133 Lokossa, Benin
[5]Laboratory of study and research on the wood material, University of Lorraine, UMR 1073, INRA, ENGREF, UHP, ENSTIB 27, BP 1041, 88 051 Epinal Cedex, France
melhyask@gmail.com

Available online at: www.isca.in, www.isca.me
Received 30th November 2024, revised 14th May 2025, accepted 13th June 2025

Abstract

Plastic bags are a common sight in West Africa, particularly in household waste. Their widespread distribution has a negative impact on the environment. Solutions need to be found to recycle them more effectively. Pyrolysis is a promising method for testing plastic bags for their thermal behavior. In this study, a laboratory test was conducted for the pyrolysis of low-density polyethylene (LDPE) in a pilot reactor. Analytical devices such as Fourier transform infrared (FTIR), gas chromatography-combustion thermal detector (GC-CTD), gas chromatography-mass spectrometry (GC-MS), and gas chromatography-flame ionization detector (GC-FID) were used to determine material and energy balances, and the composition of condensable and non-condensable gases. The results show that PE is a very good fuel in terms of energy, but its environmental impact remains undeniably negative. Therefore, the use of PE will be much more sustainable if it is mixed with other types of fuel to reduce its environmental impact.

Keywords: Poly Ethylene, Pyrolysis, Material balance, Energy balance.

Introduction

Polyethylene, one of the polyolefins, is produced by polymerizing ethylene monomers[1–3]. There are two types of PE: high-density polyethylene (HDPE) and low-density polyethylene (LDPE). Their density varies between 915 and 950 $kg.m^{-3}$. Density decreases with the length of the hydrocarbon chain, i.e. with increasing molar mass[2,4–6]. A study on PE shows that its calorific value (around 43,000 $kJ.kg^{-1}$) is almost 3 times higher than that of wood (16,200 $kJ.kg^{-1}$)[2,7–13]. PE is often used in the manufacture of plastic films, bags and sacks. It is composed of 85% carbon and 15% hydrogen[2,3,8,11]. In percentage by mass, it is composed of 99% volatile matter and 1% fixed carbon[2,10]. Polyethylene has a very low moisture content, of the order of 1 to 2% [10].

The pyrolysis of PE essentially produces hydrocarbons, carbon oxides and water. The nature and quantity of the products depends on the temperature and residence time of the gases in the heating zone[2,4,14,15]. For example, at 900°C and residence times between 0.35s and 2.5s, the alkane and alkene concentration obtained after PE pyrolysis is higher than that obtained at 800°C, [2]. However, beyond a residence time of 0.8s, there is a decrease in aliphatic hydrocarbon content, favored by cyclization, leading to the formation of aromatic hydrocarbons. Work carried out by Levendis, A. Y. & Ponagiotou, T.[16] on the pyrolysis of PE showed that this compound has a melting temperature of around 170°C and boils at temperatures of around 420°C. These results are quite different from those of Piao, M., Chu, S., Zheng, M. & Xu, X.[17], who found a melting temperature of 111°C and thermal degradation temperatures between 337°C and 447°C. This difference is due to the nature of the PE used.

The main gases released during the pyrolysis of PE are C_1 to C_4 hydrocarbons[1,17,18]. Piao, M., Chu, S., Zheng, M. & Xu, X.[19] specify that the main volatile species resulting from the thermal degradation of PE are saturated hydrocarbons, "alkenes and dienes", with chains of less than six (6) carbons. Analysis carried out by Milne, B. J. et al[20] on the products of PE pyrolysis between 780°C and 860°C, in a fluidized-bed reactor, shows that residence time has no influence on the content of certain gases such as ethane. On the other hand, there is a significant effect of residence time on the quantity of butadiene. At the same temperatures, the volume of gases produced during pyrolysis represents only 35 to 40% of the volatile matter contained in the fuel, reflecting incomplete devolatilization, the remainder being contained in solid residues. The rate of PE degradation has an impact on the production of free radicals.

The rate at which free radicals are formed increases with their stability, so the conversion rate is higher if the radicals responsible for thermal devolatilization are more stable.

Most of the hydrocarbons emitted during polyethylene pyrolysis are only slightly influenced by temperature between 800 and 1000°C, for residence times ranging from 0.6 to 2.6 seconds[21], as confirmed in Figure-1 above. However, Ouiminga, S. K. et al.[22] shows that CO emissions increase as a function of temperature between 800 and 1000°C, for residence times of 1 to 1.6 seconds.

Regarding the influence of gas residence time in the hot zone[22], during polyethylene pyrolysis, shows that NO emissions decrease for gas residence times ranging from 0.3 to 1.6 seconds, between 800 and 1000°C. For the same conditions, he also shows that carbon monoxide (CO) is an increasing function of residence time above 1 second. For the same conditions, it also shows that carbon monoxide (CO) is an increasing function of residence time above 1 second. Green and Sadrameli[21] show that the hydrocarbons CH_4 and C_2H_4, are increasing functions of residence time (between 0.6 and 2.6 seconds) and for temperatures of 800 and 850°C.

In the present study, tests were carried out on Low Density Polyethylene under pyrolitic conditions on a dedicated reactor referred to hereafter as the pyrolysis test bench. This work enabled us to assess the distribution of the various products (solid, gas and liquid) and determine their nature as a function of the operating conditions. Other papers reported the results of studies on a thermobalance located at LERMAB. These works have made it possible to describe the thermal behavior of materials and extract kinetic parameters[2,8].

Materials and Methods

The general methodology adopted in this study is presented in Figure-2.

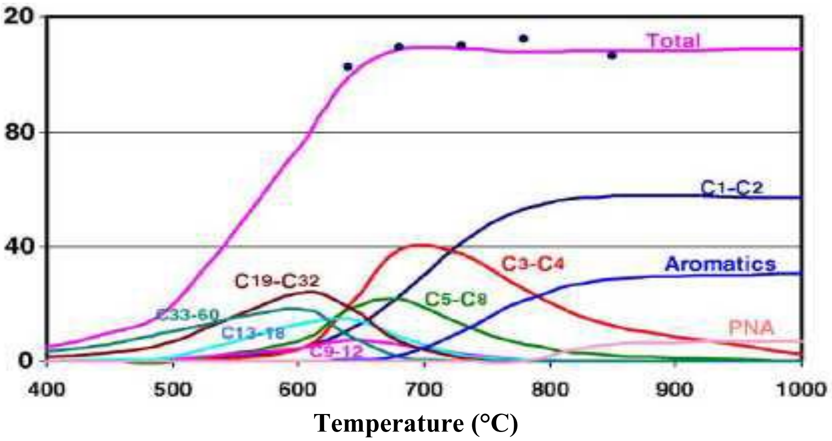

Figure-1: Rate of gas produced (%) during PE pyrolysis[21].

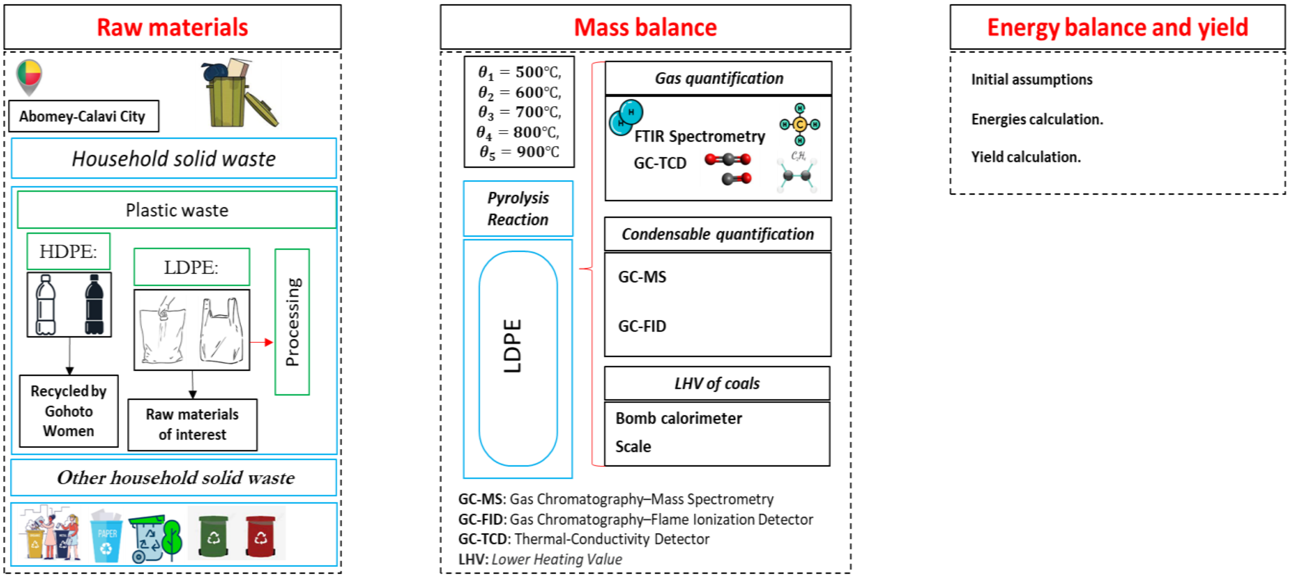

Figure-2: Guiding principle of the methodology developed.

PolyEthylene (PE): The raw materials considered in this study are the plastic waste contained in household solid waste in Benin, and more specifically in the city of Abomey-Calavi. This plastic waste consists solely of polyethylene (PE), as this is the only category of plastic found in household waste garbage cans in Benin[2,8,10,11,23]. Due to the extensive recycling of high-density polyethylene (HDPE: mineral water bottles) by so-called "Gohoto women" (a transcript from Fongbe language meaning women who buy bottles for recycling purposes), low-density polyethylene (LDPE) is the plastic waste used in the present study. The polyethylene bags were cut into small rectangular pieces measuring around 1cm^2.

Figure-3: Low Density PolyEthylene (LDPE).

Test bench and analysis devices: Reactor: This reactor, illustrated in Figure-4, consists of a cylindrical quartz tube (inner diameter 35 mm) whose temperature is controlled by an electric furnace (Thermolyne 79400), with a maximum temperature of 1100°C. The length of the hot zone is 62 cm. The furnace can operate in isothermal mode (fuel injection into the hot zone: fast pyrolysis) or in programmed temperature mode (controlled temperature ramp: slow pyrolysis).

Fuel (biomass, waste) is fed via a sample-carrying gondola, enabling the insertion of a maximum of 1 to 2g of biomass (depending on fuel density). A feed system has been developed to ensure that samples are always inserted under the same conditions (position and speed), with the insertion position controlling the residence time of the gaseous phase in the reactor's hot zone.

Sampling system: The gases generated during the test are sent to a sampling system, while the residual solid remains in the sample carrier.

The gas sampling system at the reactor outlet is adapted according to the objectives: material balance, characterization of condensable, real-time monitoring of gas composition.

For material balancing (measuring the distribution of pyrolysis products), the sampling system consists of a coil immersed in a bath maintained at -10°C, followed by a dry sawdust filter to trap condensable species (water + tar), and a tedlar sampling bag to collect dry gases prior to GC-CT analysis (Figure-5). A valve system automatically switches from "bag filling" mode during the test to "bag content analysis" mode after the test. This system enables gas bags to be filled with a flow rate that is proportional to the reactor gas outlet flow rate. Gas analysis cannot be carried out continuously, due to the long analysis time required for this type of instrument (10 minutes per measurement).

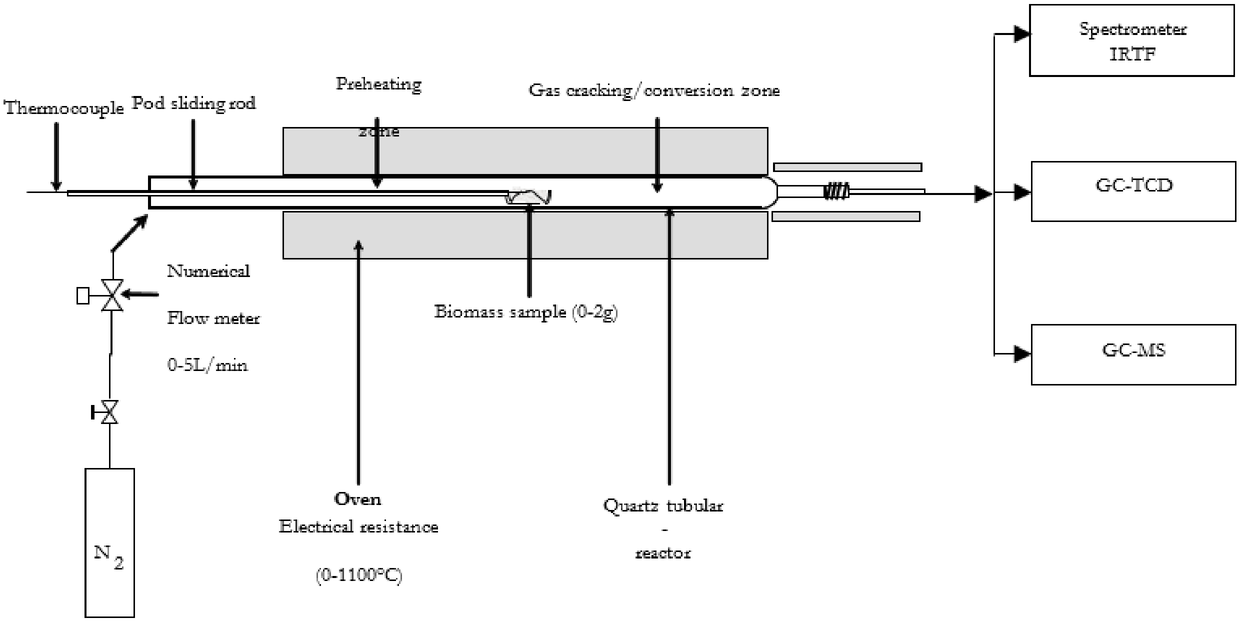

Figure-4: Schematic diagram of the experimental set-up.

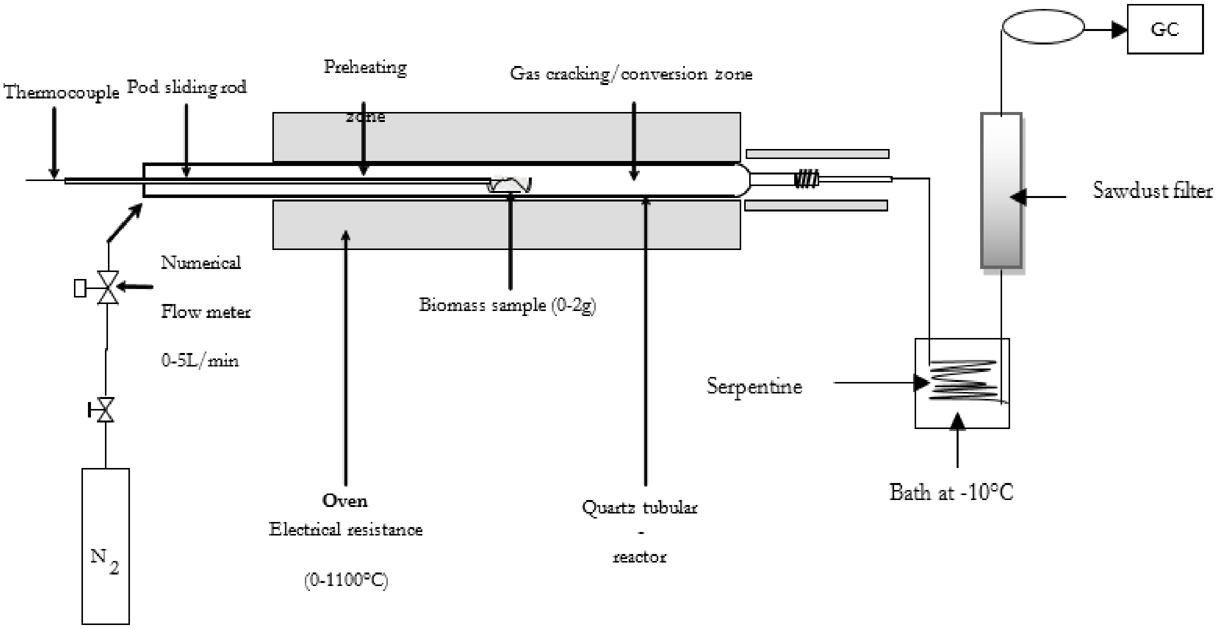

Figure-5: Experimental set-up for material balance.

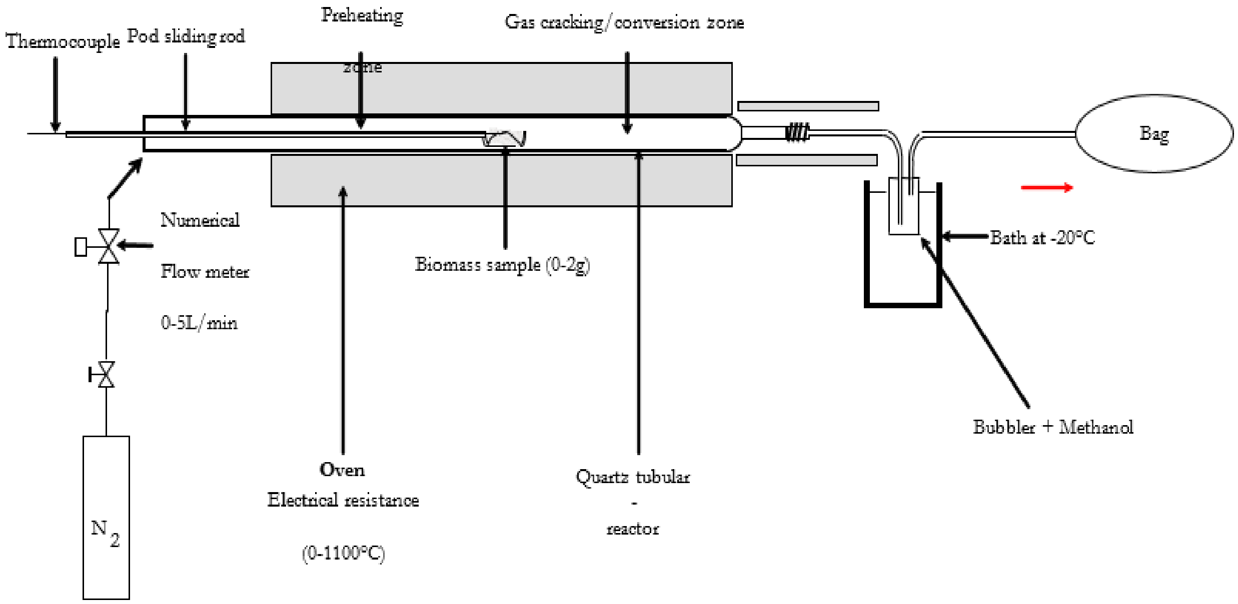

Figure-6: Experimental setup for condensable characterization.

To analyze the composition of the condensable phase, the coil + filter assembly is replaced by a bubbler maintained at -20°C (Figure-6). The solvent used is either methanol (for GC-FID measurements), or a pentane/dichloromethane mixture (2/1 by volume) for GC-MS measurements. The condensates (solvent + water + tars) collected in the bubbler are subsequently analyzed for water content (Karl-Fischer method) and tar composition (GC-MS for characterization and GC-FID for quantification of major species).

In some cases, the condensable trapping system was removed to allow all gases to be sent to a Fourier transform infrared spectrometer to identify all species formed, including pollutants, and to monitor changes in gas phase composition on a continuous basis (Figure-7). Unlike the gas chromatograph, the FTIR spectrometer enables semi-continuous measurements (every 5 seconds). The two instruments are complementary in that the latter does not measure geometric molecules such as nitrogen, oxygen or dihydrogen.

Quantification methods: We have developed methods for quantifying the different types of gases and condensable analyzed by the analysis devices used.

Gas quantification method: The volume of each gas produced during a fast pyrolysis test is obtained by using nitrogen as a tracer gas. Nitrogen is injected at a known flow rate and is neither produced nor consumed during the reaction. The volume of nitrogen trapped in the bag is calculated from the sampling time and the feed rate. The volume of compound X produced can then be obtained by a simple calculation whose expression is given below:

$$\mathrm{V(X)} = \mathrm{Q_{N_2}} \times \mathrm{t_p} \frac{\%(\mathrm{X})}{\%(\mathrm{N_2})} \quad (1)$$

$$\mathrm{m(X)} = \mathrm{V(X)} \times \frac{\mathrm{M(X)}}{\mathrm{V_o}} \quad (2)$$

$\mathbf{V(X)}$**:** The volume of compound X produced during this test (NL) l; $\mathbf{m(X)}$: the mass of compound X produced during the test (g); $\mathbf{Q_{N_2}}$ **:** carrier gas flow rate ($\mathrm{NL.min^{-1}}$); $\mathbf{t_p}$ **:** bag sampling time (min) (of the order of a minute and determined by the pyrolysis time); $\mathbf{\%(N_2)}$ **:** the percentage by volume of nitrogen in the gas analyzed, given by chromatographic analysis (%); $\mathbf{\%(X)}$: the percentage by volume of compound X in the gas analyzed (%); $\mathbf{V_o}$: Molar volume =22.4 $\mathrm{NL.mol^{-1}}$; $\mathbf{M(X)}$: the molar mass of the compound X.

Condensable quantification: The condensable species produced during pyrolysis of the plastic samples were identified by GC-MS. At the end of the analyses, the swept areas and chemical formulas of the compounds are known. As calibration of some of these compounds was not available, and could not be carried out at the time of the work, an estimation method was developed. Various condensate samples were analyzed by GC-FID and GC-MS. The calibrated species were quantified by GC-FID. The average of the ratios between the quantity (measured by GC-FID) and the area measured by GC-MS of these species was calculated and used to perform an approximate quantification of the other non-calibrated species.

Mass and energy balances: The measures required to meet the objectives are shown on the Figure-8.

The resources available to achieve the measurements listed above are presented in Table-1.

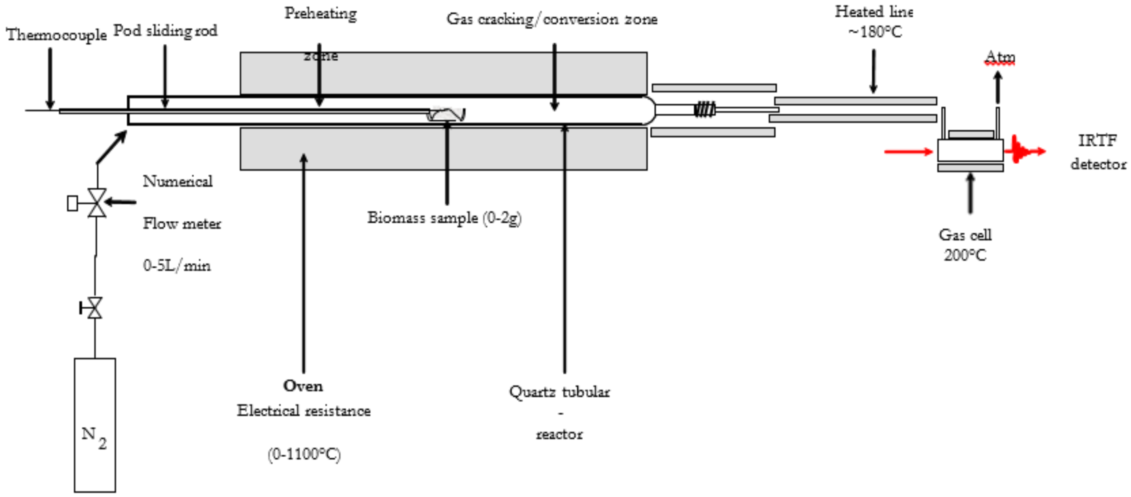

Figure-7: Experimental device for real-time monitoring of gas composition.

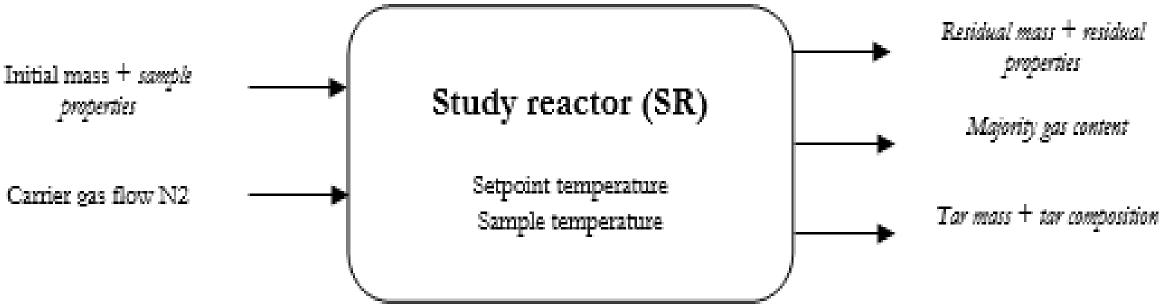

Figure-8: Reactor inlet and outlet data (in bold: set values; in italics: measured values).

Table-1: Pyrolysis measurement methods and uncertainties.

	Measurement type	Unit	Analyzer	Variation
Input measurement	Sample mass	g	Balance at 0.0001 g	0.3-1
	Elemental composition	% mass	Outside laboratory	0-100
	Sample calorific power	$kJ.kg^{-1}$	Bomb calorimeter	15000-30000
	Flow meter of N_2	$NL.min^{-1}$	Thermal mass flow meter	0.5-1
	Conservation temperature	°C	Thermocouple of the oven	250-1000
	Sample temperature	°C	Thermocouple of the oven	20-1000
Output measurement	Residual mass	g	Balance at 0.0001 g	0.3-1
	Residual elemental composition	% mass	Outside laboratory	0-100
	Residual calorific power	$kJ.kg^{-1}$	Katharometer/FTIR	15000-30000
	N_2	% volumetric	Katharometer/FTIR	35-100
	H_2	% volumetric	Katharometer/FTIR	0-50
	CO	% volumetric	Katharometer/FTIR	
	CO_2	% volumetric	Katharometer/FTIR	
	CH_4	% volumetric	Katharometer/FTIR	
	C_2H_4	% volumetric	Katharometer/FTIR	
	C_2H_6	% volumetric	Katharometer/FTIR	
	Condensable mass	mg	By weighing	0-500

Mass balance: There are two main purposes in performing mass balances. The first is to check the quality of the tests and measurements carried out, by comparing the sum of the masses of the pyrolysis products with the initial mass of the sample. According to Lavoisier, these two quantities must be identical (principle of conservation of matter). The second is to determine the distribution of pyrolysis products as a function of operating conditions, in order to simplify the choice of operating conditions for the industrial process, depending on the desired application (coal or gas production).

The mass of pyrolysis residue is weighed after the test, the mass of condensable is obtained by differential weighing of the coil and filter before and after the test, and the mass of gas (sum of the mass of all gases produced minus nitrogen) is obtained after analysis of its composition, the method being described in paragraph. The mass balance of the test is thus calculated by Equation-3.

$$\text{Mass Balance (\%)} = \sum m_s / m_i \times 100 \quad (3)$$

With m_s masses of pyrolysis products (solid residue, gas and liquid) and m_i initial mass of the sample.

Energy balance and process yield: Calculation of the process yield is essential for comparisons with other valorization methods. The experimental data collected in this section enable us to calculate the amount of energy recoverable from the solids (coals) and from the non-condensable part of the gas. The energy contained in the condensable phase cannot be calculated precisely. It cannot be considered negligible. According to Dufour, A. et al.[24] and Girods, P. et al.[25], it can account for up to 10% of total recoverable energy. In order not to overestimate the overall yield of the process, the energy contained in the condensable phase will be set at 5% of the sum of those contained in the permanent gases and the solid.

The ratio between the energy available in the pyrolysis products and that initially contained in the fuel cannot be considered as the process yield. Nevertheless, it is an interesting piece of information for comparing different experimental conditions.

Estimating process efficiency involves taking into account the energy required to feed the process and the overall efficiency of the plant, which is itself affected by temperature.

The energy required to feed the process was not measured on the plant, as it would not have been representative at all due to the small size of the reactor. It was therefore estimated. To simplify the calculation, pyrolysis is considered as athermal from a global point of view, an assumption classically used in the literature. The energy required to power the process is therefore the sum of 4 components: i. The energy required to heat the water present in the form of moisture from 20°C to 100°C; ii. The energy required to vaporize the same mass of water; iii. The energy required to heat the vapour phase from 100°C to the set temperature T; iv. The energy required to heat the dry fuel mass from 20°C to the set temperature T.

The efficiency of the pyrolysis plant depends on the size and quality of the system and the reaction temperature (heat losses increase with temperature). It is estimated at 90% for temperatures of 600 and 700°C and 85% for temperatures of 800 and 900°C.

The temperature range studied is between 600°C and 900°C in 100°C increments, so as to measure the effect of temperature and cover the different applications envisaged for pyrolysis, i.e. coal production (low temperature) and gas production (high temperature).

Results and Discussion

Mass balance: Shows the results of material balances for pyrolysed PE at various temperatures between 500 and 900°C.

Pyrolysis of PE at 500°C produced no conclusive results, as the reaction did not proceed smoothly, with only softening and melting of the fuel, resulting in the formation of a large quantity of soot in the reactor, a very small quantity of gas and a small quantity of condensable. From 600°C onwards, the level of residues resulting from pyrolysis treatment is low, corresponding to a significant degradation reaction. Between 600 and 900°C, the rate of gaseous species increases at the expense of condensable, while the yield of solids remains more or less constant. These results confirm those obtained by thermobalance by researchers[2,8,23] who revealed that, whatever the heating rate (between 5 and 50°C.min^{-}1), the degradation of PE samples was complete from 550°C onwards. It can be concluded that above 550°C, temperature increases have little effect on the primary pyrolysis reaction (heterogeneous phase transformation of the solid into gaseous species).

However, it does have an effect on the secondary reactions in the homogeneous phase, which lead to the conversion of high-molecular-weight gaseous species (condensable) into lighter species (permanent gases). At 600°C, the balance is close to 100%, but at 700°C and above, the balance is slightly less than 100%. This is due to the formation of a very high volatile matter content and the appearance of soot deposits in the reactor ducts, making residue recovery very difficult. On the other hand, at 800 and 900°C, the gas content remains more or less constant. The same trend was observed in the work carried out by Ouiminga, S. K. et al.[22].

Analysis of non-condensable gases: The results of the composition of the gas mixtures resulting from the pyrolysis of PE are given by Figure-10.

At 500°C, PE pyrolysis yielded only CO_2 and traces ofH_2. Between 600 and 900°C, the main gases are C_2H_4, le CO, le $CH_4$and CO_2. Indeed, the carbon from polyethylene pyrolysis is predominantly emitted in the form of light hydrocarbons (C_2H_4 et CH_4), a result described by Ouiminga, S. K. et al.[22,26] in his work on the degradation of PE plastic bags. The amount of C_2H_4 is very high whatever the set temperature, CO_2 decreases with temperature, while CO and the other gases show an increasing trend. The high proportion of ethylene in PE degradation gases is explained by the very chemical make-up of polyethylene which, as its name suggests, is made up of a chain of ethylene molecules that shortens during degradation, leading to the formation of a high proportion of C_2H_4 and CH_4. The high production of soot observed in these tests at temperatures above 600°C, and discussed in section, is due to the polycondensation of these species following complex radical mechanisms involving numerous intermediate species.

The low initial oxygen content of PE samples explains the low proportion of oxygenated gases such as CO_2 and CO, compared with results obtained for other samples such as wood and cardboard[2,8,27–29]. The same findings were observed by researchers[22,26] following a comparative study between the pyrolysis of millet stalks and that of plastic waste. However, using millet alone as a fuel in a pyrolysis reactor does not seem to be an adequate solution. Indeed, the gas balance shows that PE pyrolysis generates greenhouse gases such as CO_2 and CH_4. Moreover, while CO_2 decreases as a function of temperature, CH_4has the opposite tendency.

Condensable gas analysis: The results of the tar analysis (which could be identified) during PE pyrolysis are summarized in Table-2. Figure-12 shows the concentration of identified tars per unit of fuel, decreasing as a function of temperature. Examples of chromatograms from GC-MS analysis of condensable produced by PE pyrolysis at 800°C are shown in Figure-11.

These results show that condensable from PE are essentially aliphatic hydrocarbons with carbon numbers between C_8 and C_{25}. These identified compounds are in good agreement with those found by various researchers[13,30–33] in their work on HDPE (High Density PolyEthylene). Indeed, Kumar, S., & Singh, R. K.[32] identified C_9 to C_{24} alkene and alkane hydrocarbons.

The polyethylene molecular chain is made up of several carbon atoms. So, the random splitting mechanism has just as many solutions. The two intermediate chains produced are again subjected to the same mechanism, and so on until the molecules thus created are light enough to be stable under environmental conditions. It has also been observed that random scission generates a statistical distribution of the types of species produced for the same number of carbons. Thus, the probability of forming an alkene ($C = [C]_n - C$) is twice as great as the probability of forming an alkane ($C - [C]_n - C$) or a diene ($C = [C]_n = C$)[34,35]. The double bond of alkenes, which can be located to the left or right of the molecule, explains this distribution, observed in particular in Figure-13.

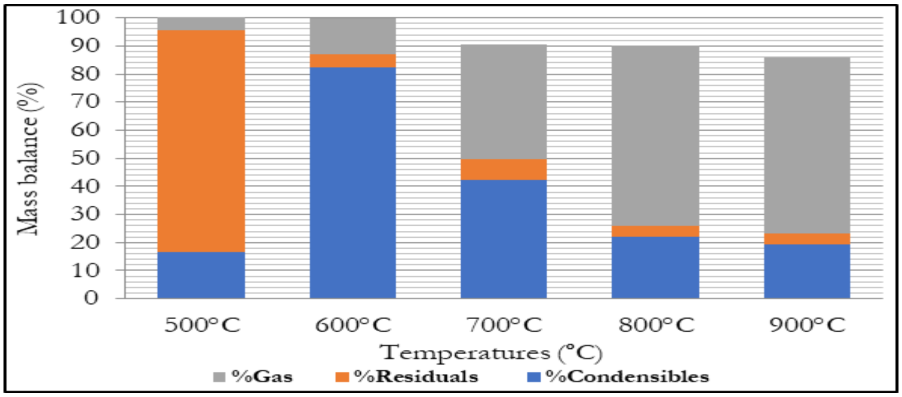

Figure-9: PE mass balance.

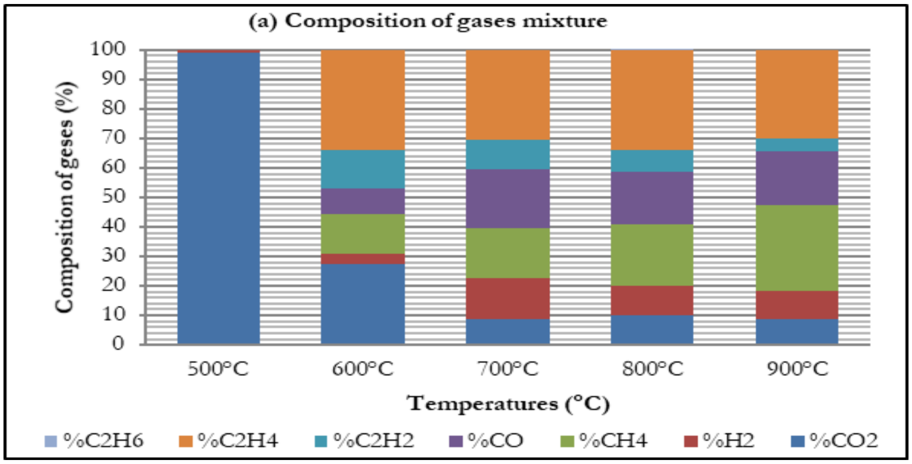

Figure-10: Importance of the gas mixture obtained after the pyrolysis of PE**.**

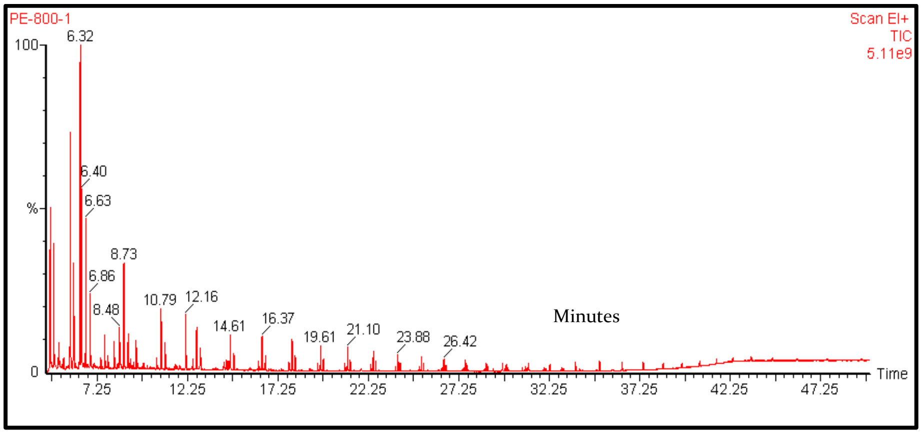

Figure-11: GC-MS of condensable from PE pyrolysis at 800°C.

Table-2: Concentrations (mg.g^{-1} fuel) of PE condensables at différent températures.

Tr (min)	Compound	Chemical formula	Concentration (mg.g^{-1})			
			600 °C	700 °C	800 °C	900 °C
4,66	1-Octene	C_8H_{16}	17,15	6,16	4,37	0,10
4,88	Octane	C_8H_{18}	7,30	3,04	3,11	0,29
6,66	1-Nonene	C_9H_{18}	15,74	6,72	3,95	0,24
6,89	Nonane	C_9H_{20}	5,30	1,99	1,87	0,10
8,77	1-Decene	$C_{10}H_{20}$	19,06	6,98	2,91	0,52
8,99	Decane	$C_{10}H_{22}$	5,31	1,60	0,99	0,19
10,82	1-Undecene	$C_{11}H_{22}$	15,95	5,03	1,71	0,62
11,04	Undecane	$C_{11}H_{24}$	6,13	1,59	0,78	0,30
12,79	1-Dodecene	$C_{12}H_{24}$	12,60	3,65	1,23	0,67
12,99	Dodecane	$C_{12}H_{26}$	6,00	1,54	0,71	0,41
14,64	1-Tridecene	$C_{13}H_{26}$	11,71	3,09	10,18	0,73
14,83	Tridecane	$C_{13}H_{28}$	5,44	1,16	0,52	0,36
16,4	1-Tetradecene	$C_{14}H_{28}$	12,15	3,13	1,08	0,65
16,57	tetradecane	$C_{14}H_{30}$	5,30	1,13	0,57	0,56
18,05	1-pentadecene	$C_{15}H_{30}$	10,63	2,75	1,05	0,80
18,21	Pentadecane	$C_{15}H_{32}$	4,93	1,02	0,53	0,39
19,62	1-Hexadecene	$C_{16}H_{32}$	8,28	2,24	0,82	0,73
19,78	Hexadecane	$C_{16}H_{34}$	4,43	0,91	0,45	0,37
21,12	1-heptadecene	$C_{17}H_{34}$	7,30	2,07	0,72	0,60
21,26	Heptadecane	$C_{17}H_{36}$	3,90	0,81	0,39	0,37
22,54	1-Octadecene	$C_{18}H_{36}$	6,51	1,90	0,64	0,62
22,67	Octadecane	$C_{18}H_{38}$	3,50	0,72	0,34	0,38
23,9	1-Nonadecene	$C_{19}H_{38}$	5,75	1,69	0,50	0,56
24,02	Nonadecane	$C_{19}H_{40}$	3,19	0,67	0,28	0,34
25,2	1-Eicosene	$C_{20}H_{40}$	4,71	1,49	0,47	0,52
25,31	Eicosane	$C_{20}H_{42}$	2,89	0,61	0,27	0,38
26,44	1-Heneicosene	$C_{21}H_{42}$	3,83	1,30	0,39	0,43
26,55	Heneicosane	$C_{21}H_{44}$	2,33	0,52	0,23	0,31
27,63	1-Docosene	$C_{22}H_{44}$	2,90	1,21	0,34	0,44
27,73	Docosane	$C_{22}H_{46}$	1,75	0,49	0,20	0,29
28,78	1-Tricosene	$C_{23}H_{46}$	2,05	1,07	0,28	0,35
28,87	Tricosane	$C_{23}H_{48}$	1,19	0,42	0,17	0,25
29,88	1-Tétracosene	$C_{24}H_{48}$	1,36	0,99	0,23	0,28
29,97	Tétracosane	$C_{24}H_{50}$	0,88	0,37	0,15	0,23
30,95	1-Pentacosene	$C_{25}H_{50}$	0,86	0,76	0,18	0,22
31,03	Pentacosane	$C_{25}H_{52}$	0,62	0,31	0,13	0,18
Total			228,93	71,13	42,74	14,80

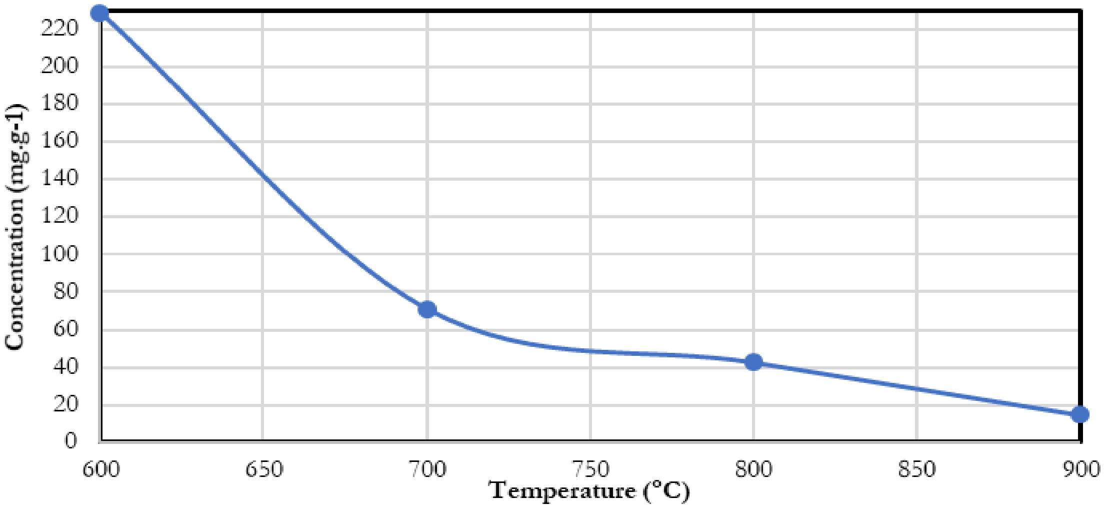

Figure-12: Concentration of tars identified during PE pyrolysis.

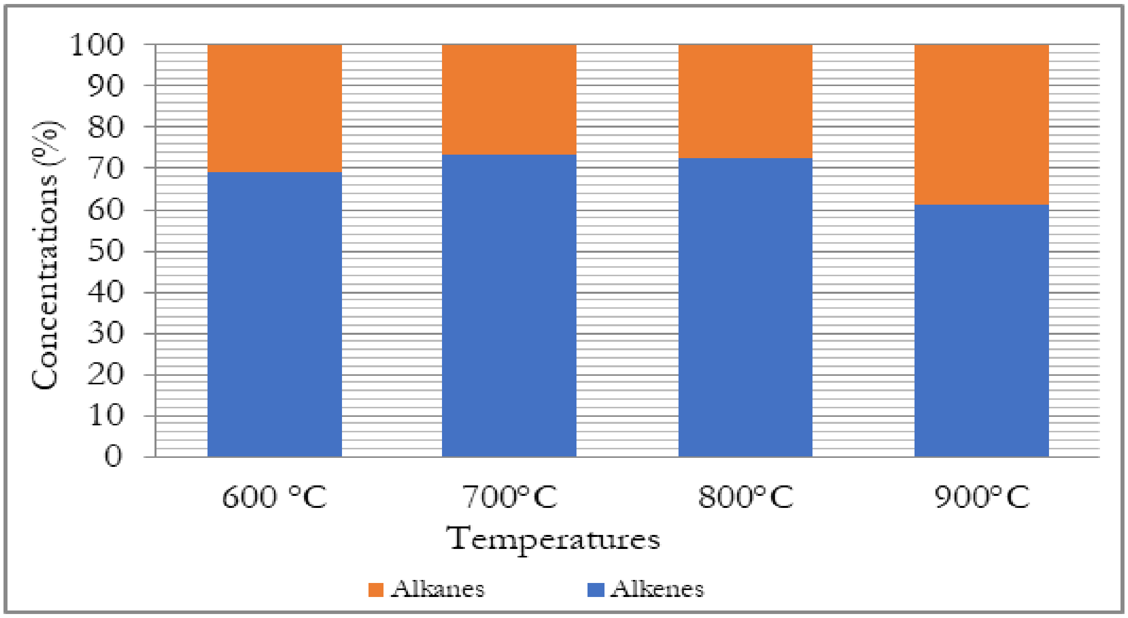

Figure-13: Quantitative breakdown of Hydrocarbons from PE.

The histogram in Figure-13 shows the quantities of hydrocarbons (alkenes and alkanes) resulting from PE pyrolysis from 600 to 900°C. This figure clearly shows that at each temperature, the quantity of alkenes is at least twice that of alkanes. These results confirm the previous assertion of the probability of formation of the hydrocarbon types identified in condensable from PE pyrolysis.

Available energy and energy conversion: Figure-14(a) and Figure-14(b) show, respectively, the variations in available energy and the energy conversion rate of products from PE pyrolysis as a function of temperature. It can be seen that between 600 and 900°C they are increasing and have the same trend as a function of temperature. In fact, these two parameters are linked solely to gas production, as neither condensable nor solid content have been considered, as the latter is only present in the form of soot in the reactor. As condensable have not been taken into account, the available Energy is very low at 600°C compared with the lower calorific value (LCV) of the PE. This is because, at this temperature, the quantity of condensable gases is high. This value increases and approaches the LCV for higher temperature values, due to the decreasing tendency of condensable, as discussed in paragraph.

It is clear from this graph that the overall energy conversion rate increases with pyrolysis temperature, suggesting that the overall efficiency of the pyrolysis process increases with temperature. However, the energy required to supply the process with energy is not taken into account here. The graph in Figure-15(a) shows the evolution of the amount of energy required to feed the process as a function of temperature, based on the assumptions given in paragraph. It can be seen that, of course, the higher the pyrolysis temperature, the higher the amount of energy required for the process.

The graph in Figure-14 (a) shows the amount of energy available in each solid (coal) and gaseous phase.

Assuming that the energy required to fuel the pyrolysis reaction in the industrial plant will be derived from the combustion of the gases produced, we need to check whether this is sufficient (compare Figure-14 (a) and Figure-15 (a)). It appears that whatever the reaction temperature, the energy available in the Gases is always greater than that required to supply the process with energy.

The overall process efficiency is estimated on the basis of the assumptions described in paragraph (energy available in each phase, energy available in condensable (estimated at 5%), energy required for the process and heat losses (85 to 90% depending on temperature). The efficiency calculated in this way is therefore representative when the gas is burned directly at the reactor outlet. However, if the gas is used in a combustion engine for cogeneration, this value is overestimated, as a purification stage (i.e. removal of condensable species) would be necessary.

The evolution of overall energy efficiency is illustrated in Figure-15(b). It increases for each type of fuel as a function of temperature. Once again, it could be concluded that the optimization of pyrolysis process conditions tends towards higher temperatures. However, it should also be noted that above 800°C, the materials used to build the reactor (stainless steel and/or refractory concrete) need to have increasingly demanding properties, so optimization from an economic point of view requires the cross-referencing of technical and economic data.

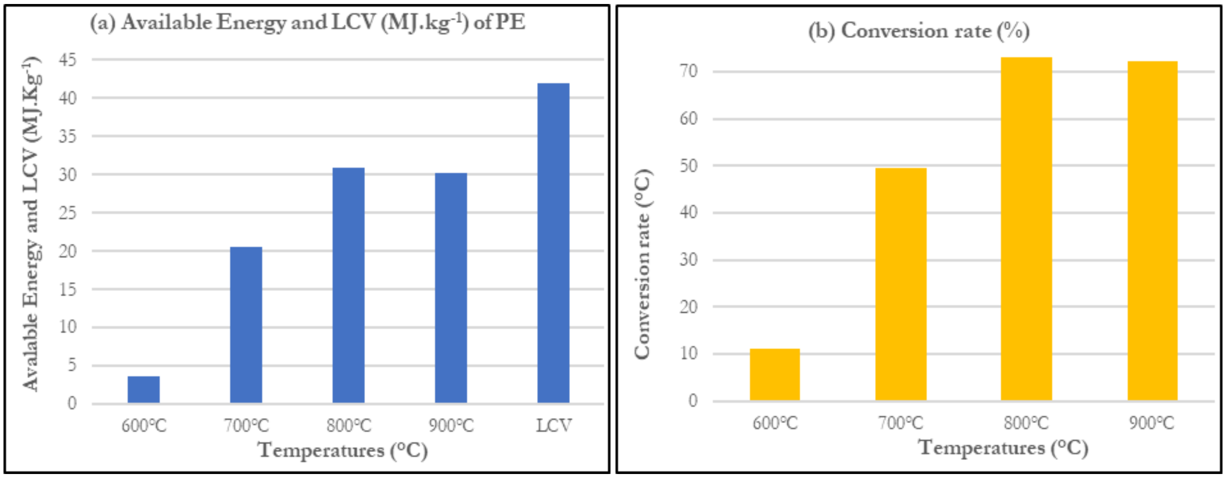

Figure-14: Available energies and energy conversion rates.

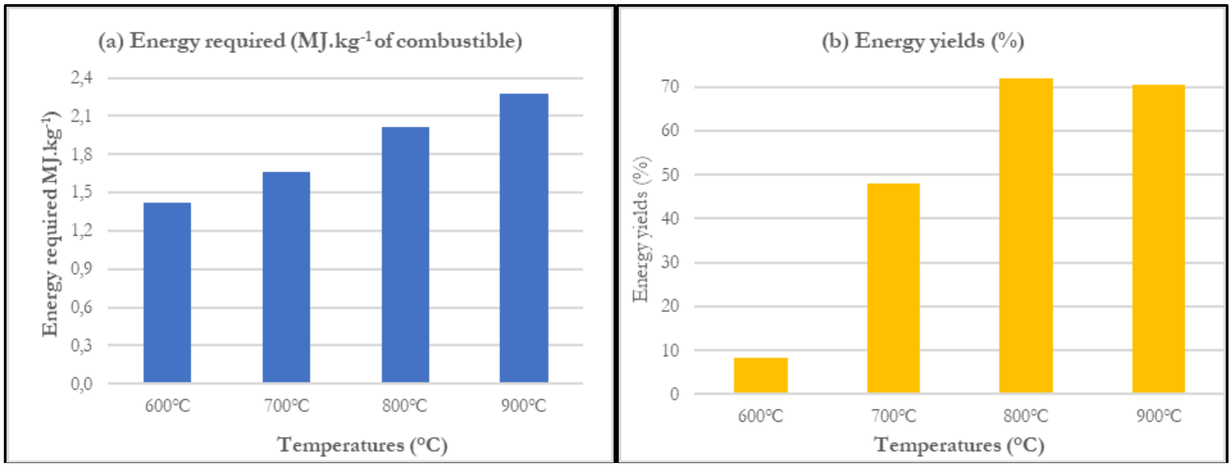

Figure-15: Energy required powering the system and energy yields.

Conclusion

The present study of PE pyrolysis took place at the Laboratory of study and research on the wood material (LERMAB), at the University of Lorraine. The studies of pyrolysis in TGA carried out by Kple, M. et al[2], Kple, M.[8] and Kplé, M. et al[36] revealed that fast pyrolysis of PE cannot take place below 500°C. The material balance showed that the increase in temperature leads to a rise in gas production at the expense of coal and condensable.

Analysis of all pyrolysis products shows that energy yield increases up to 72% at 800°C and remains substantially constant up to 900°C. It could be concluded that optimizing the conditions of the PE pyrolysis process under current conditions would lead to the highest temperatures around 800-900°C. Nevertheless, it would be far more advantageous not only in energy terms, but also environmentally, to use it in a mixture with other fuels such as cellulosic waste.

Acknowledgments

This work could not have been performed without financial support of CPER Région Lorraine for the equipment and instrumentation, financial support of Labex Arbre. The authors wish to thank these Organizations for their support.

References

1. Adeniyi, A. G., & Ighalo, J. O. (2020). Simulation of low density polyethylene (LDPE) pyrolysis and optimisation of pyro-oil yield. *International Polymer Processing*, 35(2), 229-235.
2. Kple, M., Girods, P., Fagla, B., Anjorin, M., Ziegler-Devin, I., & Rogaume, Y. (2017). Kinetic study of low density polyethylene using thermogravimetric analysis, Part 2: Isothermal study. *Waste and Biomass valorization*, 8, 707-719.
3. Kolibaba, O. B., Sokolskiy, A. I., & Gabitov, R. N. (2017). Research of the pyrolysis of municipal solid waste aimed at improving the efficiency of thermal reactors. *International Journal of Energy for a Clean Environment*, 18(2).
4. Puckins, A. I., Osipovs, P. S., & Osipovs, S. D. (2024). Method for the determination of tar produced from the pyrolysis of used tires. *International Journal of Energy for a Clean Environment*, 25(1).
5. Eren, M. R., Güneş, I., & Varol, E. A. (2024). The effect of carbonization temperature on the properties of carbonaceous material obtained from ethylene-propylene-diene-monomer (EPDM) wastes. *International Journal of Energy for a Clean Environment*, 25.
6. Adeyanju, A. A., & Manohar, K. (2023). Experimental analysis and performance of a waste plastics pyrolysis system for biofuel production. *International Journal of Energy for a Clean Environment*, 24(8).
7. Osipovs, S. D., Puckins, A. I., Mežaraupe, S., & Lazdāns, D. (2022). Determination of Pollutants in Industrial Water Used for Cooling Gases in Waste Pyrolysis Process. *International Journal of Energy for a Clean Environment*, 23(5).
8. Kple, M., Girods, P., Anjorin, M., Fagla, B., & Rogaume, Y. (2016). Thermal degradation of household solid waste in the town of Abomey-Calavi in Benin: kinetic study. *Waste and biomass valorization*, 7, 59-70.
9. Kple, M., Nonviho, G., Doto, V., Aza-Gnandji, M., Chabi, E., Bagan, G., & Houngan, A. (2022). Study of the combustion in a rotary kiln of model household waste from the city of Abomey-Calavi in Benin. *Research Journal of Engineering Sciences,* 11(3), 1-11.
10. Brandelet, B., Kple, M., Girods, P., Rose, C., Rogaume, C., & Rogaume, Y. (2016). Thermal degradation of cellulosic and plastic material: kinetic and particles determining study in combustion. *International Journal of Energy, Environment and Economics*, 24(2/3), 173.
11. Kple, M., Fagla, B. F. Z., Anjorin, M., Girods, P. & Rogaume, Y. (2016). Thermal degradation of household solid wastes with TGA: cellulosic and plastic materials. *Sylwan Journal* 36–47.
12. Łach, Ł., & Svyetlichnyy, D. (2024). Recent Progress in Heat and Mass Transfer Modeling for Chemical Vapor Deposition Processes. *Energies*, 17(13), 3267.
13. Ngusale, G. K., Oloko, M., Agong, S., & Nyakinya, B. (2017). Energy recovery from municipal solid waste. *Energy Sources, Part A: Recovery, Utilization, and Environmental Effects*, 39(16), 1807-1814.
14. Ballice, L. (2002). Classification of volatile products evolved during temperature-programmed co-pyrolysis of low-density polyethylene (LDPE) with polypropylene (PP). *Fuel*, 81(9), 1233-1240.
15. Mastral, F. J., Esperanza, E., Garcıa, P., & Juste, M. (2002). Pyrolysis of high-density polyethylene in a fluidised bed reactor. Influence of the temperature and residence time. *Journal of Analytical and Applied Pyrolysis*, 63(1), 1-15.
16. Levendis, A. Y., & Ponagiotou, T. (1991). Experimental Techniques to Study the Combustion Characteristics of two commonly found in Municipal wastes. *Municipal Waste Combustion*, 73-86.
17. Kawaguchi, O., Ohtani, T., & Kojima, H. (1997). Thermal decomposition process of a polyethylene pellet in a hot stagnation flow. *Combustion science and technology*, 130(1-6), 411-421.
18. Kiran, N., Ekinci, E., & Snape, C. E. (2000). Recyling of plastic wastes via pyrolysis. *Resources, Conservation and Recycling*, 29(4), 273-283.

19. Piao, M., Chu, S., Zheng, M., & Xu, X. (1999). Characterization of the combustion products of polyethylene. *Chemosphere*, 39(9), 1497-1512.
20. Milne, B. J., Behie, L. A., & Berruti, F. (1999). Recycling of waste plastics by ultrapyrolysis using an internally circulating fluidized bed reactor. *Journal of Analytical and Applied Pyrolysis*, 51(1-2), 157-166.
21. Green, A. E. S., & Sadrameli, S. M. (2004). Analytical representations of experimental polyethylene pyrolysis yields. *Journal of analytical and applied pyrolysis*, 72(2), 329-335.
22. Ouiminga, S. K., Rogaume, T., Sougoti, M., Commandre, J. M., & Koulidiati, J. (2009). Experimental characterization of gaseous species emitted by the fast pyrolysis of biomass and polyethylene. *Journal of Analytical and Applied Pyrolysis*, *86*(2), 260-268.
23. KPLE, M. M. (2022). Caractérisation du mélange combustible des déchets solides ménagers (DSM) de la ville d'Abomey-Calavi: Elaboration du déchet modèle. *Sciences des Structures et de la Matière*, 6(1).
24. Dufour, A., Girods, P., Masson, E., Rogaume, Y., & Zoulalian, A. (2009). Synthesis gas production by biomass pyrolysis: Effect of reactor temperature on product distribution. *International Journal of hydrogen energy*, 34(4), 1726-1734.
25. Girods, P., Dufour, A., Rogaume, Y., Rogaume, C., & Zoulalian, A. (2009). Comparison of gasification and pyrolysis of thermal pre-treated wood board waste. *Journal of Analytical and Applied Pyrolysis*, 85(1-2), 171-183.
26. Ouiminga, S. K., Rogaume, T., Daho, T., Yonli, A. H., & Koulidiati, J. (2012). Reductive and oxidative combustion of polyethylene bags: Characterization of carbonaceous and nitrogenous species. *Journal of Analytical and Applied Pyrolysis*, 98, 72-78.
27. Fayçal, B. A., Koucka, O. S., Harouna, G. I., Sadio, S. S., & Antoine, B. (2021). Caractérisation Expérimentale De Briquettes À Base de déchets papiers/cartons et étude de l'impact du liant lors de leur conception. J. P. Soaphys, 3(1), C21A04.
28. Gado, I. H., Ouiminga, S. K., Daho, T., Yonli, A. H., Sougoti, M., & Koulidiati, J. (2014). Characterization of briquettes coming from compaction of paper and cardboard waste at low and medium pressures. *Waste and Biomass Valorization*, 5, 725-731.
29. Ibrahim, H. G., Ouiminga, S. K., Yonli, A., Sanogo, O., Daho, T., & Koulidiati, J. (2018). Study of temperature fields and heavy metal content in the ash and flue gas produced by the combustion of briquettes coming from paper and cardboard waste. *Recycling*, 3(3), 32.
30. Arafat, H. A., Jijakli, K., & Ahsan, A. (2015). Environmental performance and energy recovery potential of five processes for municipal solid waste treatment. *Journal of Cleaner Production*, 105, 233-240.
31. Chen, Y. C. (2016). Potential for energy recovery and greenhouse gas mitigation from municipal solid waste using a waste-to-material approach. *Waste Management*, 58, 408-414.
32. Kumar, S., & Singh, R. K. (2011). Recovery of hydrocarbon liquid from waste high density polyethylene by thermal pyrolysis. *Brazilian journal of chemical engineering*, 28, 659-667.
33. Hasan, M. M., Rasul, M. G., Khan, M. M. K., Ashwath, N., & Jahirul, M. I. (2021). Energy recovery from municipal solid waste using pyrolysis technology: A review on current status and developments. *Renewable and Sustainable Energy Reviews*, 145, 111073.
34. Mangeot, A. (2012). Étude expérimentale et développement numérique d'une modélisation des phénomènes physicochimiques dans un propulseur hybride spatial (Doctoral dissertation, Université d'Orléans).
35. Gascoin, N., Navarro-Rodriguez, A., Gillard, P., & Mangeot, A. (2012). Kinetic modelling of high density polyethylene pyrolysis: Part 1. Comparison of existing models. *Polymer degradation and stability*, 97(8), 1466-1474.
36. Kplé, M., Nonviho, G., Chabi, E., Doto, V., Aza-Gnandji, M., Bagan, G., ... & Rogaume, Y. (2022). Kinetic study of pyrolysis of low density polyethylene using thermogravimetric analysis: Dynamic study. *RAMRes Sciences des Structures et de la Mantière*, 6(1), 106-122.